

# Enhancement of photovoltaic efficiency of phosphor doped organic solar cell by energy and electron transfer from the phosphor to C<sub>60</sub> acceptor

Dongfang Yang,<sup>1,2</sup> Wenlian Li,<sup>1,a)</sup> Bei Chu,<sup>1,b)</sup> Zisheng Su,<sup>1</sup> Junbo Wang,<sup>1,2</sup> Guang Zhang,<sup>1,2</sup> and Feng Zhang<sup>3</sup>

<sup>1</sup>Key Laboratory of Excited State Processes, Changchun Institute of Optics, Fine Mechanics and Physics, Chinese Academy of Sciences, Changchun 130033, People's Republic of China

<sup>2</sup>Graduate School of Chinese Academy of Sciences, Beijing 100039, People's Republic of China

<sup>3</sup>Key Laboratory of Optical System Advanced Manufacturing Technology, Changchun Institute of Optics, Fine Mechanics and Physics, Chinese Academy of Sciences, Changchun 130033, People's Republic of China

(Received 30 June 2011; accepted 11 October 2011; published online 7 November 2011)

About 67% increase in power conversion efficiency (PCE) of copper phthalocyanine/C<sub>60</sub> based organic solar cells was demonstrated by doping 4 wt % iridium(III)bis(3-(2-benzothiazolyl)-7-(diethylamino)-2H-1-benzopyran-2-onato-N',C<sup>4</sup>)(acetyl acetonate) (IrC<sub>6</sub>) into C<sub>60</sub> acceptor layer. The raised PCE was proved to result from the efficient photo absorption of IrC<sub>6</sub> followed by the energy and electron transfer from IrC<sub>6</sub> to C<sub>60</sub> due to the matched energy level alignment between these two species. Besides, IrC<sub>6</sub> could also increase the exciton dissociation efficiency at the active interface of the solar cells. The more detail improvement mechanisms were also discussed. © 2011 American Institute of Physics. [doi:10.1063/1.3658875]

Recently, the power conversion efficiency (PCE) of organic photovoltaic (PV) solar cells has been rapidly improved, which offered potential applications of low-cost renewable energy source. It is mainly due to the development of materials, device architectures, and processing techniques.<sup>1–6</sup> For an organic material, the absorption of photons results in the creation of bound electron-hole pairs, i.e., excitons. When the excitons diffuse to a donor-acceptor (D-A) interface, they could be dissociated into free charge carriers, i.e., holes and electrons. Finally, the holes and electrons are collected by anode and cathode, respectively.

Long exciton diffusion length ( $L_D$ ), high light absorption efficiency, efficient energy transfer, and exciton disassociation are crucial for achieving high PCE of PV solar cells. Generally, the exciton diffusion length ( $L_D$ ) of fluorescent material in a PV diode is short, i.e., in the range of 3–10 nm. As a result, some photogenerated excitons would be recombined during the diffusing process before reaching the D-A interface.<sup>7,8</sup> Long lifetime triplet excitons can be obtained by using phosphorescent material uniform layer or doping phosphor into the fluorescent active layer. In such a case, device efficiency could be enhanced by using thicker active layer and long-lived triplet excitons. On the other hand, doping phosphor into the active layer may also increase the absorption efficiency of the devices. Wade *et al.* have doped a phosphor *fac*-tris(2-phenylpyridine) iridium as a sensitizer into the PV device to enhance the  $L_D$ .<sup>9</sup> Chan *et al.*<sup>10,11</sup> have demonstrated improved PCE in their solar cells by doping fluorescent dye rubrene into the active layers.

In this work, we demonstrated enhanced efficiency of Ir-complex phosphor doped organic PV solar cells with a structure of copper phthalocyanine (CuPc)/IrC<sub>6</sub> doped C<sub>60</sub>/Bphen; here IrC<sub>6</sub> indicates iridium (III)bis(3-(2-benzothiazolyl)-7-

(diethylamino)-2H-1-benzopyran-2-onato-N',C<sup>4</sup>)(acetylacetonate) and Bphen is 4,7 diphenyl-1,10-phenanthroline. The IrC<sub>6</sub> has previously been used as a red phosphor emitter,<sup>12</sup> but it has not been used in PV solar cells. The PCE of the PV device doped with 4 wt. % IrC<sub>6</sub> was enhanced by 65%. The improvement is attributed to the effective energy and electron transfer, enhanced light absorption, and efficient exciton dissociation.

All PV devices were fabricated on pre-cleaned indium-tin-oxide (ITO) glass with a sheet resistance of 25  $\Omega$ /sq. The substrates were UV ozone treated immediately before the device fabrication. The deposition rates of organic and Al layers were controlled to 2 Å/s and 10 Å/s by vacuum evaporation at a pressure of about 10<sup>-7</sup> Torr, respectively. All organic materials were purified by sublimating for twice before used. Organic films were deposited on quartz substrates for the absorption spectra measurement with a Shimadzu UV-3101PC spectrophotometer. Current-voltage (J-V) characteristics were measured using Keithley-2400 under AM1.5 solar illuminations with an Oriol 150 W solar simulator. The singlet ( $S_1$ ) and triplet energy ( $T_1$ ) levels of CuPc, C<sub>60</sub> and 4-(dicyanomethylene)-2-*t*-butyl-6-(1,1,7,7-tetramethyl-julolidyl-9-enyl)4H-pyran (DCJTB) were cited from literatures, respectively.<sup>12–14</sup>

In order to optimize the IrC<sub>6</sub> doping content in C<sub>60</sub> acceptor, 0, 1, 2, 4, and 8 wt. % IrC<sub>6</sub> were used, respectively. Note that 4 wt. % IrC<sub>6</sub> doped PV cell presents the maximum photocurrent response. To elucidate the mechanisms of the enhanced PV response by adding 4 wt. % IrC<sub>6</sub>, a red fluorescent DCJTB doped device was also fabricated for comparison because DCJTB has a similar absorption spectrum with IrC<sub>6</sub> between 400–500 nm.<sup>13,14</sup> Three PV devices were fabricated with structures as follows:

Device-C<sub>60</sub>: ITO/CuPc (20 nm)/C<sub>60</sub> (40 nm)/Bphen (10 nm)/Al (200 nm);

Device-DCJTB: ITO/CuPc (20 nm)/C<sub>60</sub>: 4 wt. %DCJTB (40 nm)/Bphen (10 nm)/Al (200 nm);

<sup>a)</sup>Electronic mail: wllioel@yahoo.com.cn.

<sup>b)</sup>Electronic mail: beichu@163.com.

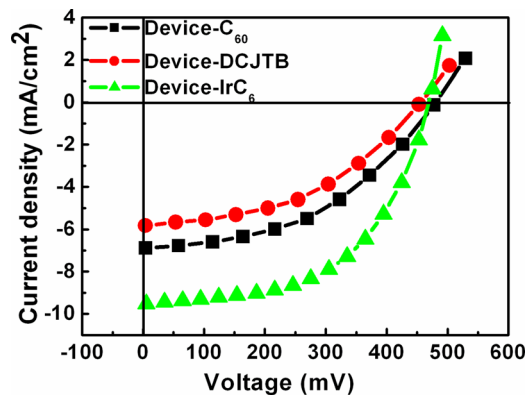


FIG. 1. (Color online) J-V characteristics of Device- $C_{60}$ , Device-DCJTB, and Device- $IrC_6$ .

Device- $IrC_6$ : ITO/CuPc (20 nm)/ $C_{60}$ : 4 wt. % $IrC_6$  (40 nm)/Bphen (10 nm)/Al (200 nm).

Figure 1 depicts the J-V characteristics of Device- $C_{60}$ , Device-DCJTB, and Device- $IrC_6$ . Table I lists the performance parameters of the three devices extracted from their J-V characteristics, respectively. The results show that an increase in photocurrent density of Device- $IrC_6$  is observed compared to that of Device- $C_{60}$  and Device-DCJTB. The short-circuit current density ( $J_{SC}$ ) of Device- $IrC_6$  is 9.5 mA/cm<sup>2</sup>, which is increased by 2.6 mA/cm<sup>2</sup> compared to Device- $C_{60}$ .

Figure 2 displays the absorption spectra of the  $C_{60}$ :  $C_{60}$ : DCJTB (4 wt. %), and  $C_{60}$ :  $IrC_6$  (4 wt. %) films, and the spectra were normalized at 266 nm. The absorption of  $C_{60}$  is assigned to electronic transitions of  $\pi \rightarrow \pi^*$  lying at 250-400 nm and  $\pi \rightarrow \pi^*$  lying at 400-700 nm, respectively,<sup>8</sup> and the latter absorption is obviously lower than that of the former. A stronger absorption of  $IrC_6$  lying at 400-500 nm region is mainly assigned to electronic transition from the ground state ( $S_0$ ) to <sup>1</sup>MLCT and to <sup>3</sup>MLCT due to the charge transfer from the metal to ligand, here <sup>1</sup>MLCT and <sup>3</sup>MLCT denote the excited singlet and triplet states, respectively. Furthermore, the absorption spectrum of  $C_{60}$ : $IrC_6$  film matches better than  $C_{60}$  film with the standard solar spectrum.<sup>15</sup> Thus, the additional absorption of  $C_{60}$ : $IrC_6$  film could directly contribute to the PV response.

On the other hand, energy transfer plays another important role in PV devices. The excited state levels of the  $C_{60}$ , DCJTB, and  $IrC_6$ , as well as the possible energy transfer processes in the PV devices are described in the inset of Fig. 3. Under illumination, singlet excitons are formed in  $C_{60}$  and  $IrC_6$  molecules, and then, they are converted to their triplet states by very fast intersystem crossing (ISC), respectively. The singlet excitons of  $C_{60}$  would be converted to longer-lived triplet excitons with a high rate driven by an

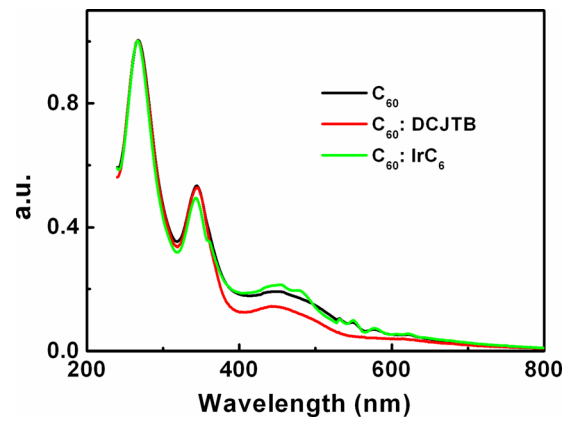


FIG. 2. (Color online) The absorption spectra of various films: neat  $C_{60}$  film, blend films of  $C_{60}$ : DCJTB, and  $C_{60}$ :  $IrC_6$  (normalized at 266 nm).

efficient spin-orbit coupling.<sup>16,17</sup> Moreover, both the  $S_1$  and  $T_1$  of  $IrC_6$  are higher than the  $S_1$  of  $C_{60}$ .<sup>18</sup> Such a matched energy level alignment would lead to energy transfer from  $IrC_6$  to  $C_{60}$ . For Device-DCJTB, only the singlet excitons were harvested and the DCJTB  $S_1$  is markedly lower than the  $S_1$  and  $T_1$  of  $C_{60}$ , indicating that the energy transfer from  $C_{60}$  to DCJTB could take place. The  $L_D$  of DCJTB singlet exciton is shorter than that of  $C_{60}$  triplet singlet exciton. As a result, the PCE of Device-DCJTB was decreased.

The decay times of the neat  $IrC_6$  and 4 wt. %  $C_{60}$  doped  $IrC_6$  films are indicated in Fig. 3. We found that the excited state lifetime of  $IrC_6$  molecules decreased from 2.57 to 0.38  $\mu$ s due to 4 wt. %  $C_{60}$  doping. The decrease of the decay time is probably the result from the energy and/or electron transfer from  $IrC_6$  to  $C_{60}$ .<sup>12</sup> So, experiments were made to confirm the carrier transfer in  $C_{60}$  and dopant blend film, here the dopant is DCJTB and  $IrC_6$ , respectively. Two devices were fabricated as follows:

Device-DCJTB/ $C_{60}$ : ITO/DCJTB (10 nm)/ $C_{60}$  (30 nm)/Bphen (10 nm)/Al

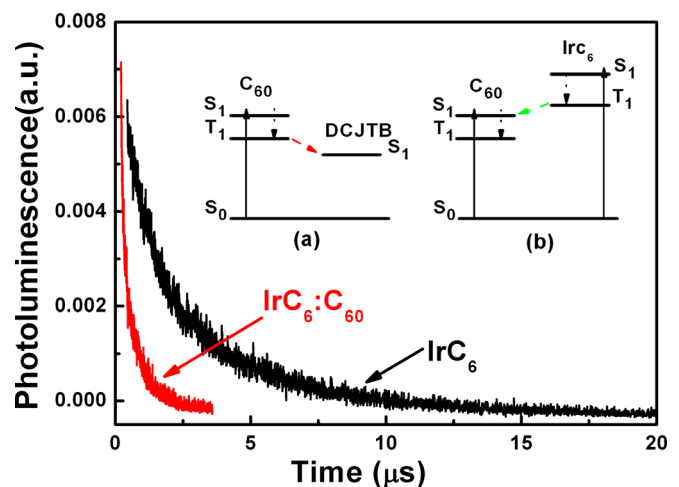


FIG. 3. (Color online) The time-resolved phosphorescence signals of  $IrC_6$  and 4 wt. %  $C_{60}$  doped  $IrC_6$  films, the decay times are indicated in the figures. Inset: the excited state levels of the DCJTB,  $IrC_6$ , and  $C_{60}$  molecules as well as the possible energy transfer processes. Solid line arrowhead: absorption, down-dot line arrowhead: ISC; Diagonal dash line arrowhead: energy transfer from  $T_1$  to  $S_1$ .

TABLE I. The PV parameter comparison between of Devices- $C_{60}$ , -DCJTB, and - $IrC_6$ . ( $V_{OC}$ : open-circuit voltage and  $FF$ : fill factor).

Device	$J_{SC}$ (mA/cm <sup>2</sup> )	$V_{OC}$ (V)	$FF$	PCE(%)
Device- $C_{60}$	6.9	0.49	0.44	1.5
Device-DCJTB	5.8	0.46	0.44	1.2
Device- $IrC_6$	9.5	0.46	0.55	2.4

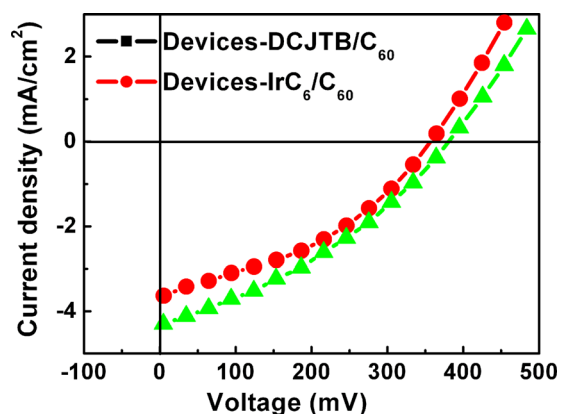


FIG. 4. (Color online) J-V characteristics of Device-DCJTB/C<sub>60</sub> and Device-IrC<sub>6</sub>/C<sub>60</sub>.

Device-IrC<sub>6</sub>/C<sub>60</sub>: ITO/IrC<sub>6</sub> (10 nm)/C<sub>60</sub> (30 nm)/Bphen (10 nm)/Al.

Figure 4 indicates the J-V characteristics of Device-DCJTB/C<sub>60</sub> and Device-IrC<sub>6</sub>/C<sub>60</sub>. It can be seen that Device-IrC<sub>6</sub>/C<sub>60</sub> also offers a higher photocurrent response than Device-DCJTB/C<sub>60</sub>, indicating that the exciton could also be efficiently dissociated at IrC<sub>6</sub>/C<sub>60</sub> interface and the IrC<sub>6</sub> layer can also act as a hole transport layer. In order to prove that the additional PV response does not come from contribution of Bphen layer, the ITO/C<sub>60</sub> (40 nm)/Bphen (10 nm)/Al device was also fabricated. The photocurrent response of C<sub>60</sub>/Bphen device can be neglected compared with that of Device-IrC<sub>6</sub>/C<sub>60</sub>. In addition, in Device-IrC<sub>6</sub>/C<sub>60</sub>, IrC<sub>6</sub> directly connects with the anode, there is not any other material to transport hole, so we can conclude that photogenerated hole can also be transported by IrC<sub>6</sub>. This result indicates that IrC<sub>6</sub> doped C<sub>60</sub> could also promote exciton dissociation, that is, IrC<sub>6</sub> could transport charge carrier in the IrC<sub>6</sub>:C<sub>60</sub> blend film at a certain extent, which could contribute to the improvement in PCE.

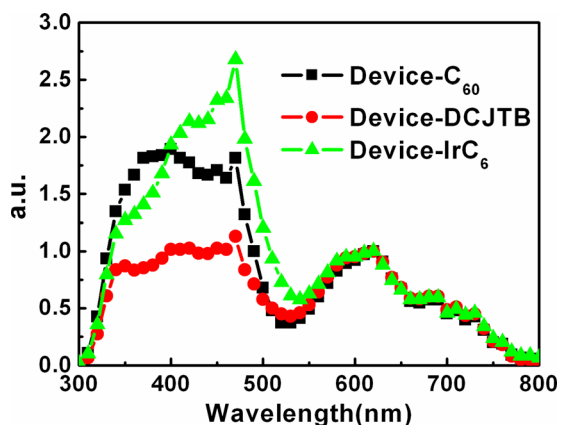


FIG. 5. (Color online) Photocurrent response curves of Device-C<sub>60</sub>, Device-DCJTB, and Device-IrC<sub>6</sub>.

Figure 5 depicts the photocurrent response curves of Device-C<sub>60</sub>, Device-DCJTB, and Device-IrC<sub>6</sub>. It is shown that the photocurrent of Device-IrC<sub>6</sub> is higher than Device-C<sub>60</sub> between 400 to 530 nm, which matches the absorption of IrC<sub>6</sub>:C<sub>60</sub>. However, the photocurrent of Device-DCJTB is declined between 350 nm to 470 nm, which is corresponding to C<sub>60</sub> absorption waveband. This phenomenon implies that C<sub>60</sub> exciton is not dissociated into carriers, in contrast its energy is transferred to DCJTB with short  $L_D$  due to the lower energy level.

In summary, we demonstrated a PCE enhancement by over 67% for organic PV solar cell with a structure of ITO/CuPc/C<sub>60</sub>: IrC<sub>6</sub> (4 wt. %)/Bphen/Al. The increase in PCE was mainly attributed to the mechanisms: IrC<sub>6</sub> could transfer its energy to C<sub>60</sub> acceptor and IrC<sub>6</sub> could also increase both the light absorption and exciton dissociation efficiency of the PV solar cell. Furthermore, the long  $L_D$  of IrC<sub>6</sub> is also an important factor. The findings indicate that organic phosphors with long lifetime and suitable energy level can be doped into organic active layers for increasing the PCE of organic PV solar cells.

This work was supported by the National Natural Science Foundation of China (Grant Nos. 60877027, 11004187, 61076047, and 61107082), Pillar Project in Bureau of science and technology of Changchun city (No. 08KZ24), and Knowledge Innovation Project of The Chinese Academy of Sciences (No. KJCX2-YW-M11).

<sup>1</sup>G. Li, V. Shrotriya, J. S. Huang, Y. Yao, T. Moriarty, K. Emery, and Y. Yang, *Nature Mater.* **4**, 864 (2005).

<sup>2</sup>B. P. Rand, J. Genoe, P. Heremans, and J. Poortmans, *Prog. Photovolt.* **15**, 659 (2007).

<sup>3</sup>J. Y. Kim, K. Lee, N. E. Coates, D. Moses, T. Q. Nguyen, M. Dante, and A. J. Heeger, *Science* **317**, 222 (2007).

<sup>4</sup>J. Peet, J. Y. Kim, N. E. Coates, W. L. Ma, D. Moses, A. J. Heeger, and G. C. Bazan, *Nature Mater.* **6**, 497 (2007).

<sup>5</sup>B. C. Thompson and J. M. J. Fréchet, *Angew. Chem., Int. Ed.* **47**, 58 (2008).

<sup>6</sup>A. Hadipour, B. de Boer, and P. W. M. Blom, *Adv. Funct. Mater.* **18**, 169 (2008).

<sup>7</sup>B. P. Rand, J. Genoe, P. Heremans, and J. Poortmans, *Prog. Photovolt.* **15**, 659 (2007).

<sup>8</sup>P. Peumans, A. Yakimov, and S. R. Forrest, *J. Appl. Phys.* **93**, 3693 (2003).

<sup>9</sup>W. A. Luhman and R. J. Holmes, *Appl. Phys. Lett.* **94**, 153304 (2009).

<sup>10</sup>M. Y. Chan, S. L. Lai, M. K. Fung, C. S. Lee, and S. T. Lee, *Appl. Phys. Lett.* **90**, 023504 (2007).

<sup>11</sup>M. Y. Chan, S. L. Lai, M. K. Fung, C. S. Lee, and S. T. Lee, *Appl. Phys. Lett.* **91**, 089902 (2007).

<sup>12</sup>S. Lamansky, P. Djurovich, D. Murphy, F. A. Razzaq, H. E. Lee, C. Adachi, P. E. Burrows, S. R. Forrest, and M. E. Thompson, *J. Am. Chem. Soc.* **123**, 4304 (2001).

<sup>13</sup>J. Qiao, Y. Qiu, L. D. Wang, L. Duan, Y. Li, and D. Q. Zhang, *Appl. Phys. Lett.* **81**, 4913 (2002).

<sup>14</sup>P. Peumans and S. R. Forrest, *Appl. Phys. Lett.* **79**, 126 (2001).

<sup>15</sup>ASTM Standard, American Society for Testing and Materials G159 (1998).

<sup>16</sup>C. S. Foote, *Top. Curr. Chem.* **169**, 347 (1994).

<sup>17</sup>R. V. Bensasson, T. Hill, C. Lambert, E. J. Land, and S. Leach, *Chem. Phys. Lett.* **201**, 326 (1993).

<sup>18</sup>M. A. Baldo, C. Adachi, and S. R. Forrest, *Phys. Rev. B* **62**, 10958 (2000).